IET Research Journals

Submission Template for IET Research Journal Papers

IET Journals
The Institution of Engineering and Technology

ISSN 1751-8644
doi: 0000000000
www.ietdl.org

Performance Improvement in Six-Phase Symmetrical Induction Motor by using Synthetic Voltage Vector based Direct Torque Control

Sohit Sharma[1]*, *Mohan Aware*[1], *Apekshit Bhowate*[1], *Emil Levi*[2]

[1] *Electrical Engineering Department, Visvesvaraya National Institute of Technology, Nagpur, India*
[2] *Liverpool John Moores University, UK*
* *E-mail: sohitee@students.vnit.ac.in*

Abstract: In this paper, direct torque control (DTC) scheme for a symmetrical six-phase induction motor by incorporating five-level torque comparator is presented. The five-level torque comparator in DTC provides the benefit of torque ripple reduction, compared to a three-level torque comparator. Adoption of five-level torque comparator generates the flux in xy-subspace which leads to flow of increased stator current. The xy-subspace flux is also not responsible for torque production. The synthetic voltage vectors are therefore developed to minimize the xy-subspace flux and thus improve performance of the symmetrical six-phase induction motor. The comparative analysis of the developed switching schemes is presented. The common mode voltage (CMV) of the drive is also taken care of by the proposed switching scheme. Experimental results are provided to verify the proposed scheme.

1 Introduction

In 1986, Takahashi and Noguchi proposed an alternative to field oriented control (FOC) for controlling the induction motor in a faster and simpler way [1]. The advantages of the direct torque control (DTC) algorithm are that neither coordinate transformation nor current control loops are required, and technique is hardly affected by parameter variations [2, 3]. The implementation of DTC algorithm for three-phase induction motors has been discussed extensively and various techniques are available to improve its performance [4-9].

In recent years, multiphase induction machines are emerging as a substitute of the three-phase induction machines because of the various inherent advantages, such as lower power per phase, lower space magneto-motive force (mmf) harmonics, higher torque density and fault tolerance property [10-12]. The first feasible phase number higher than three is five. The construction of a five-phase induction motor requires a stator with the minimum number of 20 slots in four-pole configuration [13], a slot number normally not available for three-phase machines. Hence a six-phase motor is more attractive because it can be obtained by rewinding a three-phase induction motor as a six-phase one, with the minimum number of 24 slots for four-pole topology.

The basic principle of switching table based DTC algorithm for multiphase motors is similar to the one for three-phase motors. A switching table is developed and it takes flux error, torque error, and sector number as the inputs for the selection of an appropriate voltage vector. However, this method is not directly extendable to the multiphase motors due to the presence of the extra two-dimensional subspaces (x_1y_1, x_2y_2, ...). In the multiphase machines with sinusoidal mmf distribution, electromagnetic torque production depends only on the dq-subspace and other available subspaces are responsible for losses only. When one voltage vector is selected in the dq-subspace for application, its projections in other subspaces are not zero and this deteriorates the performance of the drive [14]. Therefore, projections in other subspaces should be reduced for better drive performance. In [15], an extension of the three-phase induction motor DTC to five-phase induction motor is presented, using a two-level voltage source inverter (VSI). A DTC algorithm for five-phase induction motors supplied from a three-level neutral point clamped inverter is presented in [16], in conjunction with a seven-level torque comparator for reducing the torque ripples. The projection of the chosen vectors in xy-subspace is reduced by using the virtual voltage vectors. A generalized switching table for DTC of induction motors supplied from mutlilevel inverters is discussed in [17]. A modified switching table based DTC algorithm is proposed for reducing the current harmonics due to the presence of xy-subspace in an asymmetrical six-phase (30^o degrees spatial shift between two three-phase windings) permanent magnet synchronous machine (PMSM) [18]. In the modified switching table, selection of the voltage vectors is based on the location of the flux in xy-subspace. The incorporation of synthetic voltage vectors in DTC algorithm is developed for reducing current harmonics in dual three-phase PMSM [19]. The requirement of monitoring the stator flux in xy-subspace is eliminated with the utilization of synthetic voltage vectors. In [20], the concept of synthetic voltage vectors is extended for asymmetrical six-phase induction motor in the view of simplified implementation of the scheme by using PWM module.

When the conventional DTC algorithm is employed, the common mode voltage (CMV) generally appears in the drives; it leads to flow of common-mode current (CMC) through parasitic capacitance of the induction motor. This reduces the life expectancy of the bearings and causes unexpected tripping of ground current protection [21, 22]. Electromagnetic noise interference is also a consequence of CMV [23, 24]. To alleviate these problems, a synchronized PWM based technique has been developed for the elimination of CMV in six-phase symmetrical drives [25]. A space vector modulation based method has also been presented for symmetrical six-phase AC drives for reducing the CMV [26]. Another DTC technique, based on application of even voltage vectors in even sectors, and odd vectors in odd sectors without considering null vectors for the minimization of common-mode voltage was proposed in [27]. Therefore, torque and flux ripples are increased. The reduction of CMV with DTC algorithm for five-phase induction motor is discussed in [28], where suitable vectors are selected from the available vectors for the generation of virtual voltage vectors. This scheme additionally eliminates the xy-subspace flux as well.

A DTC scheme, similar to the conventional DTC switching scheme for three-phase induction motors, is proposed in [29] for the symmetrical six-phase induction motor supplied from a two-level VSI. Here, only large voltage vectors are applied along with a

three-level torque comparator. Therefore, it results in high torque ripples. This DTC scheme, based on the three-level torque comparator (DTC-3TC), is considered here for the comparative purpose.

As DTC algorithm for a three-phase induction motor is not directly applicable to any multiphase motor drive, it is necessary to introduce appropriate modifications and each number of phases has to be considered separately. The structure analyzed here, a symmetrical six-phase induction motor, has not been addressed previously except in [29], where a very basic DTC was considered. Hence this paper provides an addition to the existing knowledge by introducing a DTC scheme for the said stator phase disposition, based on the use of synthetic voltage vectors. Such an improved DTC, with the utilization of synthetic voltage vectors, has been developed for five-phase and asymmetrical six-phase machines in the past, but not for a symmetrical six-phase winding disposition. Since voltage vector selection has to meet simultaneously requirements for desired flux/torque error change using the first plane voltage vector projections, while at the same time keeping as close as possible to zero voltage vector projections in other planes, a detailed study of the suitable vector choices for designing the synthetic voltage vectors is provided first. It is found to be advantageous here that large voltage vectors of a symmetrical six-phase VSI map into zero voltage vectors in the xy-subspace. Next, to reduce the torque ripple, a five-level torque comparator (used previously in relation to other phase numbers but not in the context of a symmetrical six-phase induction machine's DTC) is utilized.

The implementation of a five-level torque comparator in the DTC algorithm reduces the torque ripples of the drive. This torque comparator permits utilization of the small voltage vectors of the dq-subspace. Due to the involvement of small voltage vectors, xy-subspace flux is generated. The synthetic voltage vector based five-level torque comparator scheme (DTC-5TC) is therefore developed for reducing the projections of voltage vectors in the xy-subspace. The CMV of the drive with all available switching states of the inverter is also analysed. The three-level torque comparator based switching scheme is modified to (MDTC-3TC) to eliminate the CMV of drive. The CMV, produced when the five-level torque comparator based table is used, is examined next. The redundancy of available voltage vectors provides the freedom to modify the five-level torque comparator based scheme (MDTC-5TC), so that it can simultaneously reduce the xy-subspace flux and torque ripples, and eliminate the CMV of the drive. Finally, the comparative analysis of the considered switching table based DTC techniques (DTC-3TC, MDTC-3TC, DTC-5TC and MDTC-5TC) is provided.

The paper is organized as follows. Section II summarized the modeling of symmetrical six-phase induction motor and the voltage vector mapping for a two-level VSI. The conventional DTC algorithm, based on three-level torque comparator, is further modified by introducing the five-level torque comparator. Formulation of synthetic voltage vectors for suppressing the xy-subspace flux and CMV with the available switching states is discussed in section III. Section IV provides the experimental results and is followed by the conclusions, summarized in section V.

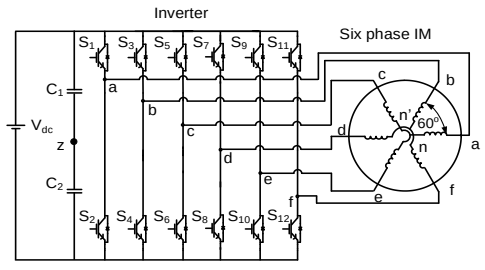

Fig. 1: *Symmetrical six-phase induction motor drive with two-level VSI supply*

2 Six-phase symmetrical induction motor model and voltage vectors of a two-level voltage source inverter (VSI)

2.1 Symmetrical Six-phase Induction Motor Modeling

Symmetrical six-phase induction motors have two three-phase windings displaced by 60 electrical degrees. The transformation matrix, based on vector space decomposition theory, transforms the six dimensional space into two two-dimensional orthogonal subspaces and two zero-sequence axes (dq, xy, $0_1 0_2$). The neutrals of both three-phase windings (n and n') are isolated, as shown Fig. 1, so that $0_1 0_2$-component equations are omitted. The symmetrical six-phase induction machine is thus modeled using:

$$[T] = \frac{1}{3}\begin{bmatrix} 1 & \cos(\frac{\pi}{3}) & \cos(\frac{2\pi}{3}) & \cos(\pi) & \cos(\frac{4\pi}{3}) & \cos(\frac{5\pi}{3}) \\ 0 & \sin(\frac{\pi}{3}) & \sin(\frac{2\pi}{3}) & \sin(\pi) & \sin(\frac{4\pi}{3}) & \sin(\frac{5\pi}{3}) \\ 1 & \cos(\frac{2\pi}{3}) & \cos(\frac{4\pi}{3}) & \cos(\frac{\pi}{2}) & \cos(\frac{8\pi}{3}) & \cos(\frac{10\pi}{3}) \\ 0 & \sin(\frac{2\pi}{3}) & \sin(\frac{4\pi}{3}) & \sin(\frac{\pi}{2}) & \sin(\frac{8\pi}{3}) & \sin(\frac{10\pi}{3}) \end{bmatrix} \tag{1}$$

The voltage equations for stator and rotor are given in dq-xy stationary reference frame as

$$\begin{aligned} v_{ds} &= R_s i_{ds} + \frac{d\psi_{ds}}{dt} \\ v_{qs} &= R_s i_{qs} + \frac{d\psi_{qs}}{dt} \end{aligned} \tag{2}$$

$$\begin{aligned} v_{xs} &= R_s i_{xs} + \frac{d\psi_{xs}}{dt} \\ v_{ys} &= R_s i_{ys} + \frac{d\psi_{ys}}{dt} \end{aligned} \tag{3}$$

$$\begin{aligned} v_{dr} = 0 &= R_r i_{dr} + \frac{d\psi_{dr}}{dt} + \omega_r \psi_{qr} \\ v_{qr} = 0 &= R_r i_{qr} + \frac{d\psi_{qr}}{dt} - \omega_r \psi_{dr} \end{aligned} \tag{4}$$

The stator and rotor flux components in the dq-xy stationary reference frame are written as

$$\begin{aligned} \psi_{ds} &= (L_{ls} + 3L_m) i_{ds} + 3L_m i_{dr} \\ \psi_{qs} &= (L_{ls} + 3L_m) i_{qs} + 3L_m i_{qr} \end{aligned} \tag{5}$$

$$\begin{aligned} \psi_{xs} &= L_{ls} i_{xs} \\ \psi_{ys} &= L_{ls} i_{ys} \end{aligned} \tag{6}$$

$$\begin{aligned} \psi_{dr} &= (L_{lr} + 3L_m) i_{dr} + 3L_m i_{ds} \\ \psi_{qr} &= (L_{lr} + 3L_m) i_{qr} + 3L_m i_{qs} \end{aligned} \tag{7}$$

where, R_s, and R_r are stator and rotor resistance, L_{ls}, and L_{lr} are stator and rotor leakage inductance, L_m is mutual inductance, i_s and i_r are stator and rotor current, and ψ_s and ψ_r are stator and rotor flux. Rotor xy voltage and flux equations are omitted since they are always zero due to the short-circuited rotor winding [10].

The electromagnetic torque (T_e) of the six-phase induction motor is given by:

$$T_e = 3P(\psi_{ds} i_{qs} - \psi_{qs} i_{ds}) \tag{8}$$

The rotor motion equations is finally:

$$\frac{d\omega_r}{dt} = \frac{P}{J}(T_e - T_l) \tag{9}$$

where, T_l is load torque, J is inertia constant, P is pole pair number, ω_r is rotor electrical speed.

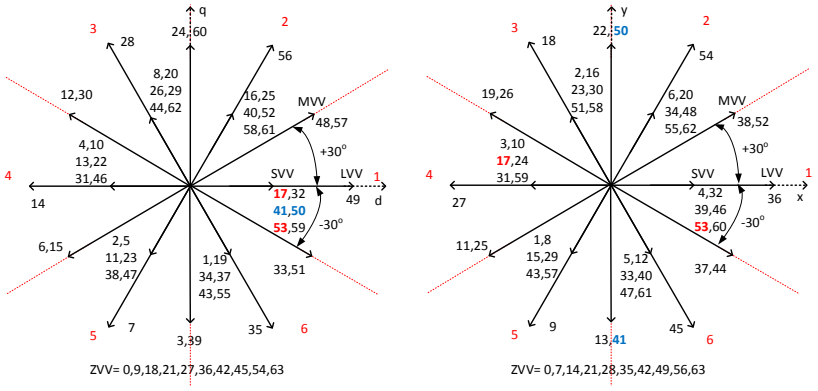

Fig. 2: *Voltage vectors in dq and xy-subspace*

2.2 Six-phase two-level voltage source inverter

A two-level VSI is shown in Fig. 1. The two switching states are possible for each leg. Therefore, there are in total $2^6 = 64$ switching states. The relationship between switching states ($S = [S_a S_b S_c S_d S_e S_f]^T$), where $S_i \in \{0,1\}$(i = a, b, c, d, e, f) and phase voltages is given by

$$\begin{bmatrix} v_a \\ v_b \\ v_c \\ v_d \\ v_e \\ v_f \end{bmatrix} = \frac{2V_{dc}}{6} \begin{bmatrix} 2 & 0 & -1 & 0 & -1 & 0 \\ 0 & 2 & 0 & -1 & 0 & -1 \\ -1 & 0 & 2 & 0 & -1 & 0 \\ 0 & -1 & 0 & 2 & 0 & -1 \\ -1 & 0 & -1 & 0 & 2 & 0 \\ 0 & -1 & 0 & -1 & 0 & 2 \end{bmatrix} \begin{bmatrix} S_a \\ S_b \\ S_c \\ S_d \\ S_e \\ S_f \end{bmatrix} \quad (10)$$

Phase voltages are represented in the two-subspaces (dq and xy) by using

$$\begin{bmatrix} v_{ds} \\ v_{qs} \\ v_{xs} \\ v_{ys} \end{bmatrix} = [T] \begin{bmatrix} v_a \\ v_b \\ v_c \\ v_d \\ v_e \\ v_f \end{bmatrix} \quad (11)$$

All the 64 voltage vectors are mapped in both subspaces, as shown in Fig. 2. For example, V_{56} vector is plotted in dq and xy-subspace by considering its binary form as the switching state (S_a = 1, S_b = 1, S_c = 1, S_d = 0, S_e = 0, S_f = 0, where 1 denotes the 'ON' state of the upper switches and 0 represents the 'ON' state of the lower switches). With reference to the mapping in the first plane, there are 6 large voltage vectors (LVV), 12 medium voltage vectors (MVV), 36 small voltage vectors (SVV), and 10 zero voltage vectors (ZVV).

3 Direct Torque Control Algorithm

The basic block diagram of the DTC scheme is presented in Fig. 3. The conventional DTC algorithm works on the basis of the selection of voltage vectors from the pre-defined switching tables. The choice of voltage vector for firing the inverter depends on the location of stator flux in dq-subspace, and output status of flux and torque hysteresis comparators. The stator flux is continuously monitored for getting the location of the stator flux in dq-subspace in terms of sectors, by means of sector identification block. The dq and xy-subspace are divided into six sectors, as shown in Fig. 2. The voltage estimator uses (10) and (11) for calculating the stator voltage components. Stator flux is estimated using (2) and the electromagnetic torque is obtained by means of (8). The two-level (2L) flux comparator is used for comparing the reference flux and actual

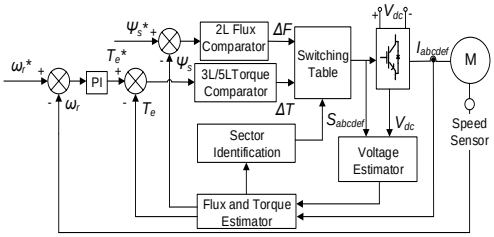

Fig. 3: *Block diagram of direct torque control algorithm*

flux. Two torque comparators, three-level (3L) torque comparator and five-level (5L) torque comparator, are considered further on.

3.1 Three-level and five-level torque comparator based switching scheme

In what is called here the conventional DTC algorithm, a three-level torque comparator is used in conjunction with 6 large voltage vectors and 2 zero voltage vectors, out of the 64 available voltage vectors. The switching table for three-level torque comparator (DTC-3TC) is shown in Table 1. The positions of selected voltage vectors are in essence the same as for the three-phase two-level VSI. The zero voltage vectors, V_0 and V_{63}, are also obtained by switching 'ON' all the lower switches and all the upper switches respectively. All vectors of this table have zero projections in the xy-subspace. Therefore, there is no need to deal separately with the xy-subspace.

The output of flux and torque comparators depends on the correlation between reference value and actual value. These relationships are, for the two-level flux comparator and three-level torque comparator, given with

$$\begin{aligned} \psi_s^* > \psi_s &\Rightarrow \Delta F = +1 \\ \psi_s^* < \psi_s &\Rightarrow \Delta F = -1 \end{aligned} \quad (12)$$

$$\begin{aligned} (T_e^* - T_e) \geq +HB &\Rightarrow \Delta T = +1 \\ -HB < (T_e^* - T_e) < +HB &\Rightarrow \Delta T = 0 \\ (T_e^* - T_e) \leq -HB &\Rightarrow \Delta T = -1 \end{aligned} \quad (13)$$

where ψ_s^* and ψ_s are the reference flux and actual flux, respectively, T_e^* and T_e are the reference torque and actual torque, respectively, and HB represents the width of the torque hysteresis band.

Table 1 Three-level torque comparator (DTC-3TC)

ΔF	ΔT	Sectors 1	2	3	4	5	6
+1	+1	V_{56}	V_{28}	V_{14}	V_7	V_{35}	V_{49}
	0	V_0	V_{63}	V_0	V_{63}	V_0	V_{63}
	-1	V_{35}	V_{49}	V_{56}	V_{28}	V_{14}	V_7
-1	+1	V_{28}	V_{14}	V_7	V_{35}	V_{49}	V_{56}
	0	V_{63}	V_0	V_{63}	V_0	V_{63}	V_0
	-1	V_7	V_{35}	V_{49}	V_{56}	V_{28}	V_{14}

The output of comparators +1, -1, and 0 demands the increase, decrease, and no change in the respective values of flux and torque. The V_{56} is selected from the switching table when the stator flux is in the first sector and there is a requirement of increase in flux and torque of the induction motor. The torque ripple of the symmetrical six-phase induction motor can be reduced by incorporating the five-level torque comparator. The available small voltage vectors are also incorporated in the switching table for obtaining the five-level torque comparator operation. The formation of the switching table is similar to DTC-3TC, but with two more torque levels. The switching table with five-level torque comparator is presented in Table 2.

The hysteresis band size of the five-level torque comparator is governed by:

$$HB_i : HB_o = |V_{SVV}| : |V_{LVV}| = 0.333V_{dc} : 0.666V_{dc} \quad (14)$$

Here, HB_i and HB_o represent the inner and outer hysteresis band, respectively. The length of small voltage vectors is half of the large voltage vectors. Therefore, if HB_o is equal to HB then HB_i is equal to $HB/2$. The operational relationships of the five-level torque comparator are given by

$$\begin{aligned} (T_e^* - T_e) \geq +HB &\Rightarrow \Delta T = +2 \\ +HB > (T_e^* - T_e) \geq +(HB/2) &\Rightarrow \Delta T = +1 \\ -(HB/2) < (T_e^* - T_e) < +(HB/2) &\Rightarrow \Delta T = 0 \\ -HB < (T_e^* - T_e) \leq -(HB/2) &\Rightarrow \Delta T = -1 \\ (T_e^* - T_e) \leq -HB &\Rightarrow \Delta T = -2 \end{aligned} \quad (15)$$

while they remain the same as in (12) for the flux comparator.

3.2 *Five-level torque comparator based switching scheme using synthetic voltage vectors*

The implementation of the switching scheme, presented in Table 2, reduces the torque ripples. However, it employs voltage vectors that have non-zero projections in the xy-subspace and hence lead to formation of the xy-subspace flux. From (3) and (6), it is observed that current flowing in this plane is only limited by leakage inductance of the machine. Due to this, high currents will flow and thus increases the losses. The xy-subspace does not contribute to the torque production. For these reasons, the synthetic voltage vectors are formed next, in order to reduce the xy-subspace flux.

3.2.1 Formulation of synthetic voltage vectors: The synthetic voltage vectors are developed by combining two small active vectors of the dq-subspace. The selected vectors have the same magnitude ($V_{dc}/3$) and angle ($\angle k\phi$) , so that the effect on torque and flux is the same with both vectors. In the xy-subspace, they map as small voltage vectors, which are out of phase. The dwell time for the selected vectors is calculated by using volt-second balancing equation in the xy-subspace. The balancing equation is written in such a manner that it neutralizes the effect in xy-subspace.

Table 2 Five-level torque comparator switching scheme

ΔF	ΔT	Sectors 1	2	3	4	5	6
+1	+2	V_{56}	V_{28}	V_{14}	V_7	V_{35}	V_{49}
	+1	V_{58}	V_{20}	V_{46}	V_5	V_{43}	V_{17}
	0	V_{42}	V_{21}	V_{42}	V_{21}	V_{42}	V_{21}
	-1	V_{43}	V_{17}	V_{58}	V_{20}	V_{46}	V_5
	-2	V_{35}	V_{49}	V_{56}	V_{28}	V_{14}	V_7
-1	+2	V_{28}	V_{14}	V_7	V_{35}	V_{49}	V_{56}
	+1	V_{20}	V_{46}	V_5	V_{43}	V_{17}	V_{58}
	0	V_{21}	V_{42}	V_{21}	V_{42}	V_{21}	V_{42}
	-1	V_5	V_{43}	V_{17}	V_{58}	V_{20}	V_{46}
	-2	V_7	V_{35}	V_{49}	V_{56}	V_{28}	V_{14}

In dq-subspace,

$$V_{svv1} = V_{dc}/3\angle k\phi = V_{svv2} \quad (16)$$

where, $\phi = 60^o$ and $k = 0, 1, 2, 3, 4, 5$ for six synthetic vectors.
In xy-subspace,

$$\begin{aligned} V_{svv1} &= V_{dc}/3\angle(180 + j\phi) \\ V_{svv2} &= V_{dc}/3\angle(360 + j\phi) \end{aligned} \quad (17)$$

where, $\phi = 60^o$ and $j = 0, 2, 4, 6, 8, 10$ for six synthetic vectors.

$$V_{svv1}T_1 - V_{svv2}T_2 = 0 \quad (18)$$

$$T_s = T_1 + T_2 \quad (19)$$

where, T_s is the sampling time and T_1, T_2 are the times of application, calculated for the respective vectors. From (18) and (19), it is observed that $T_1 = T_2 = T_s/2$. In one sampling time, both selected voltage vectors are applied for half of the time. All the developed synthetic voltage vectors are mapped in the dq and xy-subspaces as shown in Fig. 4. The projection of synthetic vectors in xy-subspace is zero. For SV_{40-58} vector, value of both V_{svv1} and V_{svv2} in the dq-subspace is $V_{dc}/3\angle 60$ (here, k of (16) is 1). Projection in xy-subspace is given by (17) as $V_{svv1} = V_{dc}/3\angle 300$ and $V_{svv2} = V_{dc}/3\angle 480$ ($j = 2$ for the second synthetic vector). Therefore, they cancel each other leading to zero total projection in the xy-subspace.

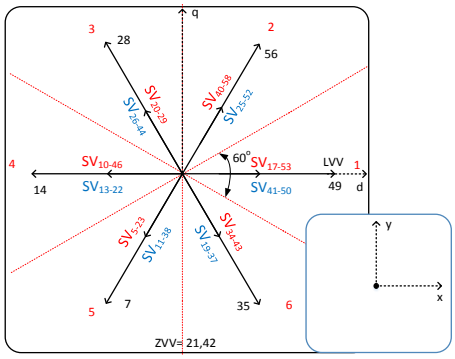

Fig. 4: *Voltage vectors of DTC-5TC and MDTC-5TC scheme in both subspaces (dq and xy)*

Table 3 Five-level torque comparator with SVVs (DTC-5TC)

		Sectors					
ΔF	ΔT	1	2	3	4	5	6
+1	+2	V_{56}	V_{28}	V_{14}	V_7	V_{35}	V_{49}
	+1	SV_{40-58}	SV_{20-29}	SV_{10-46}	SV_{5-23}	SV_{34-43}	SV_{17-53}
	0	V_{42}	V_{21}	V_{42}	V_{21}	V_{42}	V_{21}
	-1	SV_{34-43}	SV_{17-53}	SV_{4-58}	SV_{20-29}	SV_{10-46}	SV_{5-23}
	-2	V_{35}	V_{49}	V_{56}	V_{28}	V_{14}	V_7
-1	+2	V_{28}	V_{14}	V_7	V_{35}	V_{49}	V_{56}
	+1	SV_{20-29}	SV_{10-46}	SV_{5-23}	SV_{34-43}	SV_{17-53}	SV_{40-58}
	0	V_{21}	V_{42}	V_{21}	V_{42}	V_{21}	V_{42}
	-1	SV_{5-23}	SV_{34-43}	SV_{17-53}	SV_{40-58}	SV_{20-29}	SV_{10-46}
	-2	V_7	V_{35}	V_{49}	V_{56}	V_{28}	V_{14}

Table 4 CMV in symmetrical six-phase induction motor drive with two-level VSI

Number of VVs	VVs	CMV
1	0	$-V_{dc}/2$
1	63	$+V_{dc}/2$
6	1,2,4,8,16,32	$-V_{dc}/3$
6	31,47,55,59,61,62	$+V_{dc}/3$
15	3,5,6,9,10,12,17,18,20,24,33,34,36,40,48	$-V_{dc}/6$
15	15,23,27,29,30,39,43,45,46,51,53,54,57,58,60	$+V_{dc}/6$
20	7,11,13,14,19,21,22,25,26,28,35,37,38,41,42,44,49,50,52,56	0

3.2.2 Switching scheme based on synthetic voltage vectors: The switching scheme based on synthetic voltage vectors is given in Table 3. The selection of vectors is similar as in the switching scheme presented in Table 2. The difference is that, instead of small vectors, synthetic voltage vectors are applied, which are capable of reducing the xy-subspace flux. However, torque ripples remain unaltered.

3.3 Modified three-level (MDTC-3TC) and five-level torque comparator (MDTC-5TC) based switching scheme for CMV elimination

In the above developed switching schemes for the DTC algorithm, CMV of the drive is not considered. Therefore, CMV due to all available voltage vectors is explored in order to reduce its value to zero. The DTC-3TC switching table is modified to MDTC-3TC for eliminating the CMV. For the five-level torque comparator, MDTC-5TC switching scheme is proposed by considering synthetic voltage vectors for the elimination of CMV.

3.3.1 CMV in six-phase symmetrical induction motor with two-level VSI: The CMV of six-phase symmetrical induction motor drive with two-level VSI is given with

$$V_{cmv} = \frac{v_{az} + v_{bz} + v_{cz} + v_{dz} + v_{ez} + v_{fz}}{6} \tag{20}$$

which is the average of the CMV of the two individual three-phase windings, as shown by

$$V_{cmv} = \frac{V_{cmv-I} + V_{cmv-II}}{2} \tag{21}$$

where,
$V_{cmv-I} = (v_{az} + v_{cz} + v_{ez})/3$ and
$V_{cmv-II} = (v_{bz} + v_{dz} + v_{fz})/3$

The V_{cmvI} and V_{cmvII} are common-mode voltage of the first and the second three-phase winding, respectively, in terms of pole voltages ('z' is the mid-point of the dc bus). When the lower switch of the inverter is 'ON' then pole voltage of that phase is -$V_{dc}/2$ and pole voltage is +$V_{dc}/2$ when the upper switch is 'ON'. For example, 54^{th} ([1 1 0 1 1 0]) switching state generates pole voltage for each phase as v_{az} = +$V_{dc}/2$, v_{bz} = +$V_{dc}/2$, v_{cz} = -$V_{dc}/2$, v_{dz} = +$V_{dc}/2$, v_{ez} = +$V_{dc}/2$, and v_{fz} = -$V_{dc}/2$, which gives the overall CMV of +$V_{dc}/6$. Different switching states generate different pole voltages and value of CMV is obtained by using (20). The CMV obtained due to all 64 switching states is presented in Table 4.

3.3.2 Switching scheme for eliminating the CMV: From the Table 4, it is observed that all large voltage vectors are not responsible for the CMV generation. In the DTC-3TC switching table, large and zero voltage vectors are adopted. The zero voltage vectors (V_0, V_{63}) produce $\pm V_{dc}/2$ CMV. Therefore, for this switching table, generated CMV has three-levels (+$V_{dc}/2$, 0, -$V_{dc}/2$). When the zero voltage vectors (V_0, V_{63}) are replaced by (V_{21}, V_{42}) vectors, then CMV of the drive is eliminated. The modified switching table for three-level torque comparator (MDTC-3TC) is presented in Table 5.

In the DTC-5TC, zero voltage vectors (V_{21}, V_{42}) are employed. Therefore, CMV due to large and zero voltage vectors is zero. But for small vectors, CMV is $\pm V_{dc}/6$. The developed MDTC-5TC switching scheme incorporates those voltage vectors which have zero CMV. A total of 20 voltage vectors are available, which provide zero CMV, as shown in Table 4. These 20 voltage vectors are composed of 6 large, 12 small, and 2 zero vectors. The projection of large and zero voltage vectors in xy-subspace is zero. But the small

Table 5 Three-level torque comparator (MDTC-3TC)

		Sectors					
ΔF	ΔT	1	2	3	4	5	6
+1	+1	V_{56}	V_{28}	V_{14}	V_7	V_{35}	V_{49}
	0	V_{42}	V_{21}	V_{42}	V_{21}	V_{42}	V_{21}
	-1	V_{35}	V_{49}	V_{56}	V_{28}	V_{14}	V_7
-1	+1	V_{28}	V_{14}	V_7	V_{35}	V_{49}	V_{56}
	0	V_{21}	V_{42}	V_{21}	V_{42}	V_{21}	V_{42}
	-1	V_7	V_{35}	V_{49}	V_{56}	V_{28}	V_{14}

Table 6 Five-level torque comparator with SVVs (MDTC-5TC) for zero CMV

		Sectors					
ΔF	ΔT	1	2	3	4	5	6
+1	+2	V_{56}	V_{28}	V_{14}	V_{7}	V_{35}	V_{49}
	+1	SV_{25-52}	SV_{26-44}	SV_{13-22}	SV_{11-38}	SV_{19-37}	SV_{41-50}
	0	V_{42}	V_{21}	V_{42}	V_{21}	V_{42}	V_{21}
	-1	SV_{19-37}	SV_{41-50}	SV_{25-52}	SV_{26-44}	SV_{13-2}	SV_{11-38}
	-2	V_{35}	V_{49}	V_{56}	V_{28}	V_{14}	V_{7}
-1	+2	V_{28}	V_{14}	V_{7}	V_{35}	V_{49}	V_{56}
	+1	SV_{26-44}	SV_{13-22}	SV_{11-38}	SV_{19-37}	SV_{41-50}	SV_{25-52}
	0	V_{21}	V_{42}	V_{21}	V_{42}	V_{21}	V_{42}
	-1	SV_{11-38}	SV_{19-37}	SV_{41-50}	SV_{25-52}	SV_{26-44}	SV_{13-22}
	-2	V_{7}	V_{35}	V_{49}	V_{56}	V_{28}	V_{14}

vectors are mapped as medium voltage vectors in the xy-subspace. For reducing the flux in the xy-subspace, synthetic voltage vectors are formed by above stated principle, and are plotted in Fig. 4. The projection of these synthetic vectors in xy-subspace is also zero. The final switching scheme for DTC with five-level torque comparator for CMV elimination is presented in Table 6.

4 Experimental Results

The developed switching schemes (MDTC-3TC, DTC-5TC and MDTC-5TC) for the DTC are verified on the laboratory prototype of symmetrical six-phase induction motor of 1.5 kW and compared with conventional switching scheme (DTC-3TC). The experimental set-up is shown in Fig. 5 and its parameters are presented in Table 7. Texas instrument's digital signal processor is used

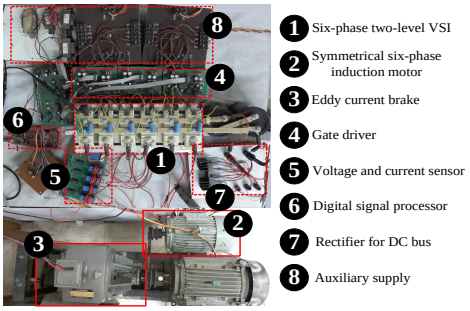

Fig. 5: *Experimental rig*

Table 7 System parameters

Parameters	Values
Dc bus voltage	200 V
Pole pairs	2
Fundamental frequency	50 Hz
Rated power	1.5 kW
Rated flux	0.35 Wb
R_s, R_r	5.17 Ω, 2.3 Ω
L_{ls}, L_{lr}	20.8 mH
L_m	215 mH

(TMS320F28377S) for the implementation of the algorithm. The Hall effect voltage and current sensors and a high resolution encoder are used for sensing the feedback signals.

An eddy current brake is used to load the motor. The sampling frequency of 10 kHz is maintained in all the switching schemes. The results are collected at the speed of 1200 rpm, in closed loop operation. The dq-subspace flux for all switching schemes is maintained at 0.35 Wb. The current flowing through the machine windings under no-load is presented in Fig. 6(a) with DTC-3TC and MDTC-3TC, and its values are 1.18 A (RMS) and 1.12 A (RMS), respectively. The Fig. 6(b) shows the dq-subspace flux. The xy-subspace flux with the corresponding switching tables is shown in Fig. 6(c). When the five-level torque comparator based switching scheme is employed, current flowing through the motor winding is as shown in Fig. 7.

Due to the presence of small voltage vectors, xy-subspace flux is generated. As a consequence, 2.1 A (RMS) current is drawn by the machine. As the xy-subspace flux can be reduced by using the synthetic voltage vectors for the DTC-5TC and MDTC-5TC schemes, current flowing through the windings is reduced to 1.17 A (RMS) and 1.21 A (RMS), respectively. This is confirmed with results

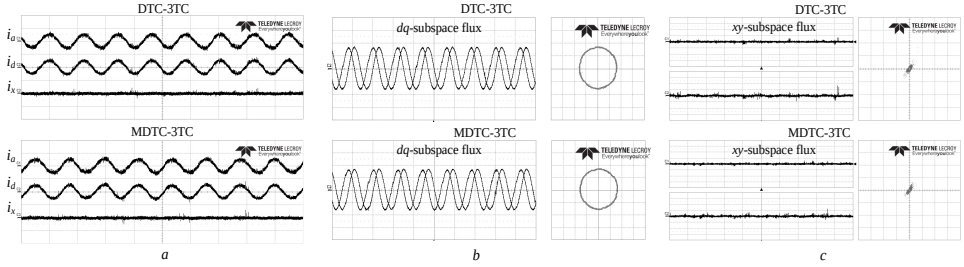

Fig. 6: *Experimental results for DTC-3TC and MDTC-3TC*
a C1= a-phase current, C2= d-axis current, C3= x-axis current [3 A/div, 20 ms/div]
b C3= d-flux, C2= q-flux [0.2 Wb/div, 20 ms/div]
c C1= x-flux, C2= y-flux [0.04 Wb/div, 20 ms/div]

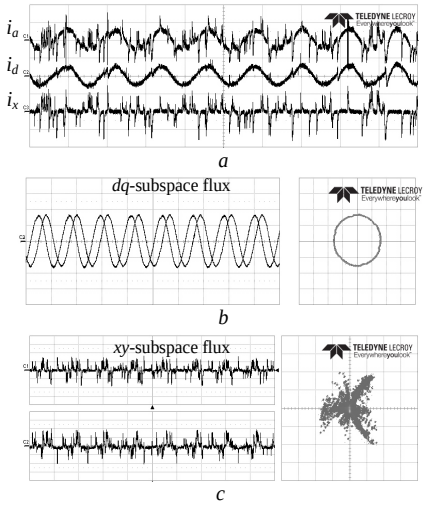

Fig. 7: *Experimental results for five-level torque comparator by using Table 2 (without synthetic voltage vectors)*
a C1= a-phase current, C2= d-axis current, C3= x-axis current [3 A/div, 20 ms/div]
b C3= d-flux, C2= q-flux [0.2 Wb/div, 20 ms/div]
c C1= x-flux, C2= y-flux [0.04 Wb/div, 20 ms/div]

shown in Fig. 8, where stator current, dq and xy-subspace flux for DTC-5TC and MDTC-5TC are shown. In no-load operation, current drawn by the five-level torque comparator based DTC without synthetic voltage vectors is very high, compared to other switching schemes, due to the presence of xy-subspace flux. Therefore it is not feasible to apply load on the motor without reducing the xy-subspace flux, if overload is to be avoided.

The step speed response is observed next, for DTC-3TC, MDTC-3TC, DTC-5TC and MDTC-5TC, with loading of 2 Nm load. The initial speed of the motor is 600 rpm. The step change of 600 rpm is commanded; therefore due to action of the speed controller, speed of motor increases to 1200 rpm, as shown in Fig. 9(a). The dynamic response for the load disturbance is presented in Fig. 9(b) and 9(c). The speed of the motor is governed with the 1200 rpm reference and the initial load is 2 Nm. The load of 5 Nm is then applied to the motor, with the resulting dynamics illustrated in Fig. 9(b). The speed of the motor momentarily reduces due to step loading. The PI controller comes in action and motor regains its speed. The torque response when motor is unloaded from 4 Nm to 2 Nm load is further presented in Fig. 9(c) and similar, but with inverse speed change sign, effects are observed.

The torque ripples for the DTC-3TC and MDTC-3TC are higher due to the three-level torque comparator. The torque ripples are reduced by incorporating the five-level torque comparator, as confirmed by Fig. 9. Both algorithms (DTC-5TC and MDTC-5TC) use five-level torque comparator based table and therefore both have similar torque ripples. The torque ripples are calculated by using (22) as suggested in [19]

$$T_{e\_ripple} = \sqrt{\frac{1}{n}\sum_{i=1}^{n}(T_{e\_i} - T_{e\_avg})^2} \tag{22}$$

where, T_{e_i} and T_{e_avg} are instantaneous and average value of the estimated torque. The calculated values of torque ripples are presented in Table 8 for the respective switching schemes. Here it is observed that selection of voltage vectors under the same torque comparator does not affect the torque ripples. However, employment of the five-level torque comparator significantly reduces the torque ripples when compared to the three-level comparator, by up to 44%. The variation of torque ripples and average switching frequency with change in load is observed at speed of 1200 rpm; next, variation of the torque ripples and average switching frequency with change in rotor speed at 2 Nm load is also investigated. The results are presented in Fig 10. It is observed that, in the whole range, torque ripples are almost constant with either three-level or five-level torque comparator. In the MDTC-3TC, average switching frequency reduces with respect to DTC-3TC due to replacement of zero voltage vectors V_0, V_{63} with V_{21}, V_{42}. It is observed that implementation of synthetic voltage vectors for the five-level torque comparator scheme increases the average switching frequency of the drive and MDTC-5TC has also slightly higher average switching frequency compared to DTC-5TC.

The CMV of the drive with different switching scheme is observed and presented in Fig. 11. In the symmetrical six-phase motor two three-phase windings are present. The CMV due to both individual three-phase windings is shown along with its resultant value. In the conventional DTC (DTC-3TC), CMV of $\pm V_{dc}/2$ is generated due to the involvement of (V_0, V_{63}) voltage vectors. In the MDTC-3TC, all employed voltage vectors are applied in such a

Table 8 Comparison of torque ripples for different switching schemes at 4 Nm load with speed of 1200 rpm

Switching scheme	DTC-3TC	MDTC-3TC	DTC-5TC	MDTC-5TC
Torque ripple (Nm)	0.311	0.307	0.175	0.179

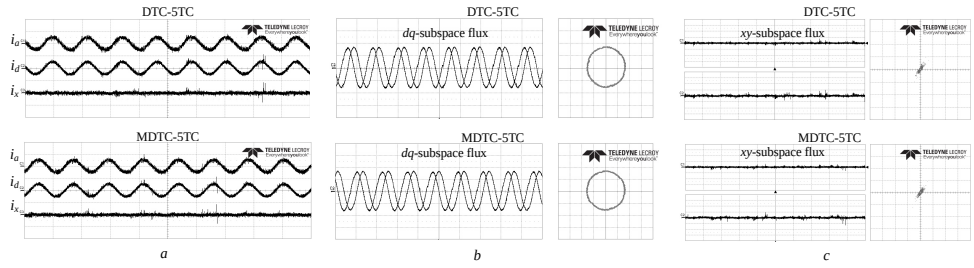

Fig. 8: *Experimental results for DTC-5TC and MDTC-5TC*
a C1= a-phase current, C2= d-axis current, C3= x-axis current [3 A/div, 20 ms/div]
b C3= d-flux, C2= q-flux [0.2 Wb/div, 20 ms/div]
c C1= x-flux, C2= y-flux [0.04 Wb/div, 20 ms/div]

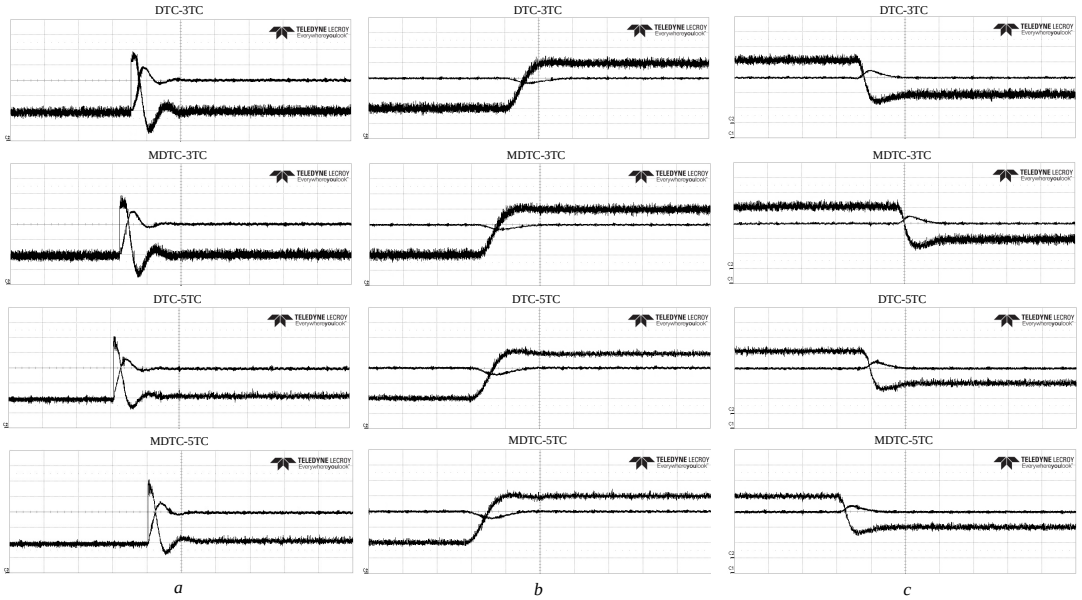

Fig. 9: *Transient response for DTC-3TC, MDTC-3TC, DTC-5TC, and MDTC-5TC switching scheme*
a Step speed response [C1= Speed (300 rpm/div, 500ms/div), C2= Torque (1 Nm/div, 500ms/div)]
b Torque response with increment in load [C1= Speed (300 rpm/div, 200ms/div), C2= Torque (1 Nm/div, 200ms/div)]
c Torque response with decrement in load [C1= Speed (300 rpm/div, 200ms/div), C2= Torque (1 Nm/div, 200ms/div)]

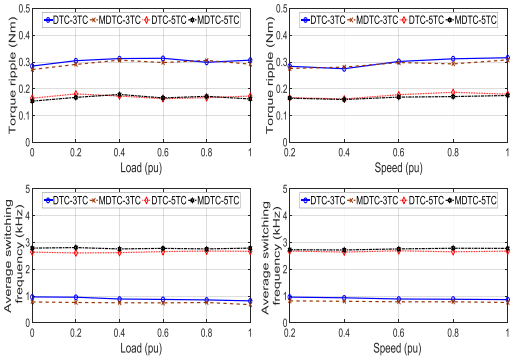

Fig. 10: *Torque ripple and average switching frequency variation with change in load and rotor speed*

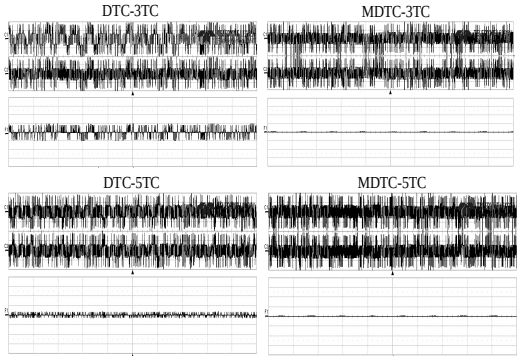

Fig. 11: *CMV of drive with DTC-3TC, MDTC-3TC, DTC-5TC, and MDTC-5TC swiching schemes [Trace 1 - C1= CMV-I, Trace 2 - C2= CMV-II (50 V/div, 20ms/div), Trace 3 - F1= CMV (100 V/div, 20ms/div)]*

manner that they generate opposite CMV in two windings. Therefore, resultant CMV is zero. However, in individual windings CMV has two values $\pm V_{dc}/6$ and $\pm V_{dc}/2$. The DTC-5TC table uses voltage vectors which generate CMV of $\pm V_{dc}/6$. Therefore, corresponding synthetic voltage vectors also generate the same CMV with three-levels ($+V_{dc}/6$, 0, $-V_{dc}/6$). The voltage vectors of DTC-5TC scheme are modified in MDTC-5TC scheme to eliminate the CMV of the drive.

5 Conclusion

In this paper, a direct torque control method using synthetic voltage vectors is introduced for a symmetrical six-phase induction motor drive. The conventional switching table of DTC (DTC-3TC) employs only large and zero voltage vectors. The five-level torque comparator based switching scheme is therefore proposed, which utilizes the available small voltage vectors of the dq-subspace. The projection of these vectors in xy-subspace is reduced by developing synthetic voltage vectors. The incorporation of synthetic voltage vectors in the scheme with five-level torque comparator effectively reduces the xy-subspace flux and the torque ripples by up to 44%. By a proper selection of the voltage vectors, CMV of the drive is also eliminated. The conventional three-level torque comparator (DTC-3TC) based table is modified to MDTC-3TC by replacing the redundant zero voltage vectors for eliminating the CMV, with

an additional benefit of reduced average switching frequency. Similarly, such voltage vectors are selected which impress zero CMV for the formulation of synthetic voltage vectors. Therefore, proposed switching table (MDTC-5TC) effectively minimizes the xy-subspace flux, reduces the torque ripples and eliminate the CMV of the drive at the expense of an increase in the average switching frequency. The experimental results are presented to validate the performance improvements realized with the MDTC-5TC switching scheme.

6 References

1 Takahashi I. and Noguchi T.: 'A New Quick-Response and High-Efficiency Control Strategy of an Induction Motor', *IEEE Trans. Ind. Appl.*, 1986, **22**, (5), pp. 820-827

2 Buja G. S. and Kazmierkowski M. P.: 'Direct torque control of PWM inverter-fed AC motors - a survey', *IEEE Trans. Ind. Electron.*, 2004, **51**, (4), pp. 744-757

3 Kumar R. H., Iqbal A. and Lenin N. C.: 'Review of recent advancements of direct torque control in induction motor drives - a decade of progress', *IET Power Electron.*, 2018, **11**, (1), pp. 1-15

4 Habetler T. G., Profumo F., Pastorelli M. and Tolbert L. M.: 'Direct torque control of induction machines using space vector modulation', *Conf. Record of the 1991 IEEE Ind. Appl. Society Annual Meeting*, Dearborn, MI, 1991, pp. 428-436

5 Jun-Koo Kang and Seung-Ki Sul: 'New direct torque control of induction motor for minimum torque ripple and constant switching frequency', *IEEE Trans. Ind. Appl.*, 1999, **35**, (5), pp. 1076-1082

6 Kyo-Beum Lee, Joong-Ho Song, Ick Choy and Ji-Yoon Yoo: 'Torque ripple reduction in DTC of induction motor driven by three-level inverter with low switching frequency', *IEEE Trans. Power Electron.*, 2002, **17**, (2), pp. 255-264

7 Shyu K., Lin J., Pham V., Yang M. and Wang T.: 'Global Minimum Torque Ripple Design for Direct Torque Control of Induction Motor Drives', *IEEE Trans. Ind. Electron.*, 2010, **57**, (9), pp. 3148-3156

8 Zaid S. A., Mahgoub O. A. and El-Metwally K. A.: 'Implementation of a new fast direct torque control algorithm for induction motor drives', *IET Elect. Power Appl.*, 2010, **4**, (5), pp. 305-313

9 Cirrincione M., Pucci M., Vitale G. and Cirrincione G.: 'A new direct torque control strategy for the minimization of common-mode emissions', *IEEE Trans. Ind. Appl.*, 2006, **42**, (2), pp. 504-517

10 Levi E., Bojoi R., Profumo F., Toliyat H. A. and Williamson S.: 'Multiphase induction motor drives - a technology status review', *IET Elect. Power Appl.*, 2007, **1**, (4), pp. 489-516

11 Barrero F. and Duran M. J.: 'Recent Advances in the Design, Modeling, and Control of Multiphase Machines-Part I', *IEEE Trans. Ind. Electron.*, 2016, **63**, (1), pp. 449-458

12 Duran M. J. and Barrero F.: 'Recent Advances in the Design, Modeling, and Control of Multiphase Machines-Part II', *IEEE Trans. Ind. Electron.*, 2016, **63**, (1), pp. 459-468

13 Levi E.: 'Multiphase Electric Machines for Variable-Speed Applications', *IEEE Trans. Ind. Electron.*, 2008, **55**, (5), pp. 1893-1909

14 Pandit J. K., Aware M. V., Nemade R. V. and Levi E.: 'Direct Torque Control Scheme for a Six-Phase Induction Motor With Reduced Torque Ripple', *IEEE Trans. Power Electron.*, 2017, **32**, (9), pp. 7118-7129

15 Huangsheng Xu, Toliyat H. A. and Petersen L. J.: 'Five-phase induction motor drives with DSP-based control system', *IEEE Trans. Power Electron.*, 2002, **17**, (4), pp. 524-533

16 Tatte Y. N. and Aware M. V.: 'Torque Ripple and Harmonic Current Reduction in a Three-Level Inverter-Fed Direct-Torque-Controlled Five-Phase Induction Motor', *IEEE Trans. Ind. Electron.*, 2017, **64**, (7), pp. 5265-5275

17 Brando G., Dannier A., Del Pizzo A., Rizzo R. and Spina I.: 'Generalised look-up table concept for direct torque control in induction drives with multilevel inverters', *IET Elect. Power Appl.*, 2015, **9**, (8), pp. 556-567

18 Hoang K. D., Ren Y., Zhu Z.-Q., and Foster M.: 'Modified switching-table strategy for reduction of current harmonics in direct torque controlled dual three- phase permanent magnet synchronous machine drives', *IET Elect. Power Appl.*, 2015, **9**, (1), pp. 10-19

19 Ren Y. and Zhu Z. Q.: 'Enhancement of Steady-State Performance in Direct-Torque-Controlled Dual Three-Phase Permanent-Magnet Synchronous Machine Drives With Modified Switching Table', *IEEE Trans. Ind. Electron.*, 2015, **62**, (6), pp. 3338-3350

20 Pandit J. K., Aware M. V., Nemade R. and Tatte Y.: 'Simplified Implementation of Synthetic Vectors for DTC of Asymmetric Six-Phase Induction Motor Drives', *IEEE Trans. Ind. Appl.*, 2018, **54**, (3), pp. 2306-2318

21 Julian A. L., Oriti G., and Lipo T. A.: 'Elimination of common-mode voltage in three-phase sinusoidal power converters', *IEEE Trans. Power Electron.*, 1999, **14**, (5), pp. 982-989

22 Kalaiselvi J. and Srinivas S.: 'Bearing currents and shaft voltage reduction in dual-inverter-fed open-end winding induction motor with reduced CMV PWM methods', *IEEE Trans. Ind. Electron.*, 2015, **62**, (1), pp. 144-152

23 Cacciato M., Consoli A., Scarcella G. and Testa A.: 'Reduction of common-mode currents in PWM inverter motor drives', *IEEE Trans. Ind. Appl.*, 1999, **35**, (2), pp. 469-476

24 Rahman K., Al-Emadi N., Iqbal A. and Rahman S.: 'Common mode voltage reduction technique in a three-to-three phase indirect matrix converter', *IET Elect. Power Appl.*, 2018, **12**, (2), pp. 254-263

25 Oleschuk V., Bojoi R., Griva G. and Profumo F.: 'Symmetrical six-phase drives with common-mode voltage elimination based on synchronized PWM', *2007 International Aegean Conf. on Electrical Machines and Power Electron.*, Bodrum, 2007, pp. 800-806

26 Correa M. B. R., Jacobina C. B., da Silva C. R., Lima A. M. N. and da Silva E. R. C.: 'Six-phase AC drive system with reduced common-mode voltage', *IEEE International Electric Machines and Drives Conf.*, Madison, WI, USA, 2003, pp. 1852-1858

27 Cirrincione M., Pucci M., Vitale G., and Cirrincione G.: 'A new direct torque control strategy for the minimization of common-mode emissions', *IEEE Trans. Ind. Appl.*, 2006, **42**, (2), pp. 504-517

28 Tatte Y. N. and Aware M. V.: 'Direct Torque Control of Five-Phase Induction Motor With Common-Mode Voltage and Current Harmonics Reduction', *IEEE Trans. Power Electron.*, 2017, **32**, (11), pp. 8644-8654

29 Alcharea R., Kianinezhad R., Nahid-Mobarakeh B., Betin F. and Capolino G. A.: 'Direct torque control for six-phase symmetrical induction machines', *2008 34th Annual Conf. of IEEE Ind. Electron.*, Orlando, FL, 2008, pp. 3090-3095